Electronic Supplementary Information

for

Azidomethyl-Bisoxadiazol-Linked-1,2,3-Triazole-(ABT)-Based Potential Liquid Propellant and Energetic Plasticizer†

Sohan Lal†, Richard J. Staples‡, Jean'ne M. Shreeve*†

†Department of Chemistry, University of Idaho, Moscow, Idaho 83844-2343

‡Department of Chemistry, Michigan State University, East Lansing, Michigan 48824

To whom correspondence should be addressed. E-mail: jshreeve@uidaho.edu. Fax: +1-208-885-9146

Table S01. Computed Zero-Point Energies (ZPE), Thermal Correction (H_T), Total Energies (E_0), and enthalpy of formation of compound **5.**

Compound	E_0 (a.u)	ZPE (a.u)	H_T (a.u)	$\Delta H_f°$ (g) kJ/mol	$\Delta H_{vap}°$ kJ/mol	$\Delta H_f°$ (s) kJ/mol
5	-1167.128457	0.175851	0.020242	1051.07	40.86	1010.21
A	-320.0499145	0.114728	0.007981	173.63	----	----
B	-339.8913334	0.101693	0.007764	-16.42	----	----
CH_4	-40.3796224	0.044793	0.003812	-74.60[a]	----	----
CH_3-CH_3	-79.5716305	0.074610	0.004428	-84.00	----	----
CH_3N_3	-203.607680	0.050250	0.005430	296.54	----	----

[a] Obtained at G2 level. [b]Calculated using isodesmic equation as shown in Fig. S1. [c]Calculated using $\Delta H_{vap} = 0.090 \times T_b/kJmol^{-1}K^{-1}$.

The gas-phase enthalpy of formation $\Delta_f H°(g)$ was predicted using Gaussian 03 program[1] according to isodesmic equation as shown in Figure S1.

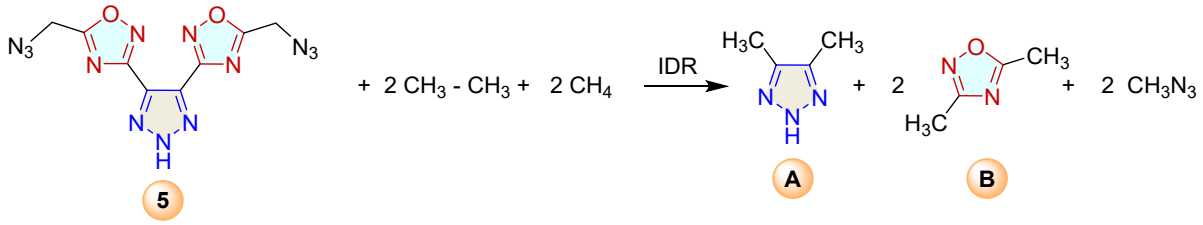

Fig. S01: Isodesmic reaction for compound **5**.

Subsequently, solid-phase enthalpy of formation $\Delta_f H°$ (s) were calculated by using equation 1.[2-5]

$$\Delta_f H°(s) = \Delta_f H°(g) - \Delta H_{vap} \quad (1)$$

Where, $\Delta_f H°(s)$ is solid phase enthalpy of formation, $\Delta_f H°(g)$ is gas phase enthalpy of formation and ΔH_{vap} is the enthalpy of vaporization.

The enthalpy of vaporization was estimated using equation 2.[5]

$$\Delta H_{vap} = 0.090 \times T_b/kJmol^{-1}K^{-1} \quad (2)$$

where, T_b, is the boiling point (bp) of compound.

The bond dissociation energy (BDE) of compound **5** was estimated according to following equation 3.

$$BDE\ [AB] = E_0\ [A.] + E_0\ [B.] - E_0\ [AB] \quad (3)$$

where, BDE [AB] is bond dissociation energy and E_0 [A.] and E_0 [B.] are the energies of individual homolytic part and E_0 [AB] is the total energy of the individual molecule.

Table S02. The standard enthalpy of combustion $\Delta H_f^\circ{}_{(combust)}$ for the title compounds was calculated by following equation **5**.

$\Delta_f H^\circ_{(combust)} = \Sigma\Delta_f H^\circ_{(products)} - \Sigma\Delta_f H^\circ_{(reactants)}$	(4)
5 $= C_8H_5N_{13}O_2\ (s) + 8.25O_2\ (g) \longrightarrow 8CO_2\ (g) + 2.5H_2O\ (g) + 6.5N_2\ (g)$	(5)
TNT $= C_7H_5N_3O_6\ (s) + 5.25O_2\ (g) \longrightarrow 7CO_2\ (g) + 2.5H_2O\ (g) + 1.5N_2\ (g)$	(6)
RDX $= C_3H_6N_6O_6\ (s) + 1.5\ O_2\ (g) \longrightarrow 3CO_2\ (g) + 3H_2O\ (g) + 3N_2\ (g)$	(7)

The standard enthalpy of formation for CO_2 ($\Delta H_{f\ (CO2)}$ = -393.51 kJmol^{-1}); H_2O ($\Delta H_{f\ (H2O)}$ = -243.015 kJmol^{-1}).

Table S03. Comparison of the ratio of positive and negative ESPs and the surface area of ESPs of compounds and positive variance, total variance, balance of charges and product of total variance and balance of charges.

Compounds	A_{tot}[a] Å^2	A_{pos}[b] Å^2	A_{neg}[c] Å^2	$ratio_{pos}$ (%)	$ratio_{neg}$ (%)	$\sigma^2{}_{tot}\upsilon$[d] (kcal/mol)
5	327.98	165.04	162.94	50.32	49.68	36.91
TNT	221.89	128.42	93.47	57.88	42.12	22.48
RDX	209.49	116.77	92.72	55.74	44.26	27.29

[a]SA_{tot} = Total surface area. [b]SA_{pos} = positive surface area. [c]SA_{neg} = Negative surface area. [d]Ratio of positive surface area [e] [d]Ratio of negative surface area. [g]Product of total variance and balance of charges.

Experimental section

General Methods

All reagents and solvents were used as received unless otherwise specified (AKSci, Sigma-Aldrich, Acros Organics, VWR). The densities of the new compounds were measured at 25 °C with a Micromeritics Accupyc II 1340 gas pycnometer. Thermal stabilities (melting and decomposition points) were measured by heating individual samples from 35 to 400 °C at a heating rate of 5 °C min^{-1} on a Differential Scanning Calorimeter (DSC, TA Instruments

Company, Model: Q2000) and thermogravimetric analysis (TGA, TA Instruments Company, Model: Q50). The FTIR spectra were recorded using KBr plates on a Thermo Nicolet AVATAR 370 spectrometer. ^{1}H and ^{13}C NMR spectra were obtained on a 500 MHz (Brucker) nuclear magnetic resonance spectrometer operating at 500.19 and 125.77 MHz, respectively, using DMSO-d_6 as the solvent and locking solvent. As external standards, the chemical shifts are given relative to tetramethylsilane (^{1}H, ^{13}C). Elemental analyses (C, H, N) were performed on a Vario Micro cube Elemental Analyser.

The crystals of compound **4·DMSO**, was mounted on a nylon loop with Paratone oil on an XtaLAB Synergy, Dualflex, HyPix diffractometer at 100 K. The structure was solved with the ShelXT[6-10] solution program using dual methods and Olex2.[10] The model was refined with ShelXL[6-10] using full matrix least squares minimization on F2.

Caution!

The compounds studied are potentially high-energy materials. Therefore, it is strongly recommended that they should be synthesized in only small amounts and handled with extreme care.

2*H*-1,2,3-Triazole-4,5-dicarbonitrile (2). Compound **2** was synthesized according to the literature report.[2] Diaminomaleonitrile **1** (10.80 g, 100 mmol, 1 equiv.) was stirred in HCl solution (4N HCl, 150 mL) at 0 °C, and an aqueous solution of $NaNO_2$ (7.60 g 10.2 g, 110 mmol, 1.10 equiv.) in water (80 mL) was added dropwise by maintaining to the reaction temperature 0 °C. The reaction mixture was stirred for 4 hours. The precipitate was removed by filtration, and the aqueous solution was extracted with ethyl acetate (5 × 100 mL). The organic layers were combined and dried over anhydrous Na_2SO_4 and the solvent was evaporated under vacuum resulted a pale-yellow solid **2**. Yield: 11.66 g, 98%. DSC (5 °C min^{-1}): T_m (onset) 146 °C, T_d (onset) 233 °C; ^{1}H NMR (500.19 MHz, DMSO-d_6): δ 14.68 (s, 1H); ^{13}C NMR (125.77 MHz, DMSO-d_6): δ 110.3, 124.0.

5-Dihydroxy-2*H*-1,2,3-triazole-4,5-bis(carboximidamide) (3). Compound **2** (1.191 g, 10.0 mmol) was dissolved in ethanol (50 mL) and hydroxylamine monohydrate (1.454 g, 22.0

mmol) was added. Then the resulting reaction mixture was held under reflux for 4 h. The reaction solution was brought to room temperature and ethanol was evaporated and the resulting precipitate was washed with cold water to give compound **3** (1.778 g, 96%) as a colourless solid. T_d (onset) 255 °C; ^{1}H NMR (500.19 MHz, DMSO-d_6): δ 9.94 (s, 2H), 6.79 (s, 4H) ; ^{13}C NMR (125.77 MHz, DMSO-d_6): δ 134.3, 147.7.

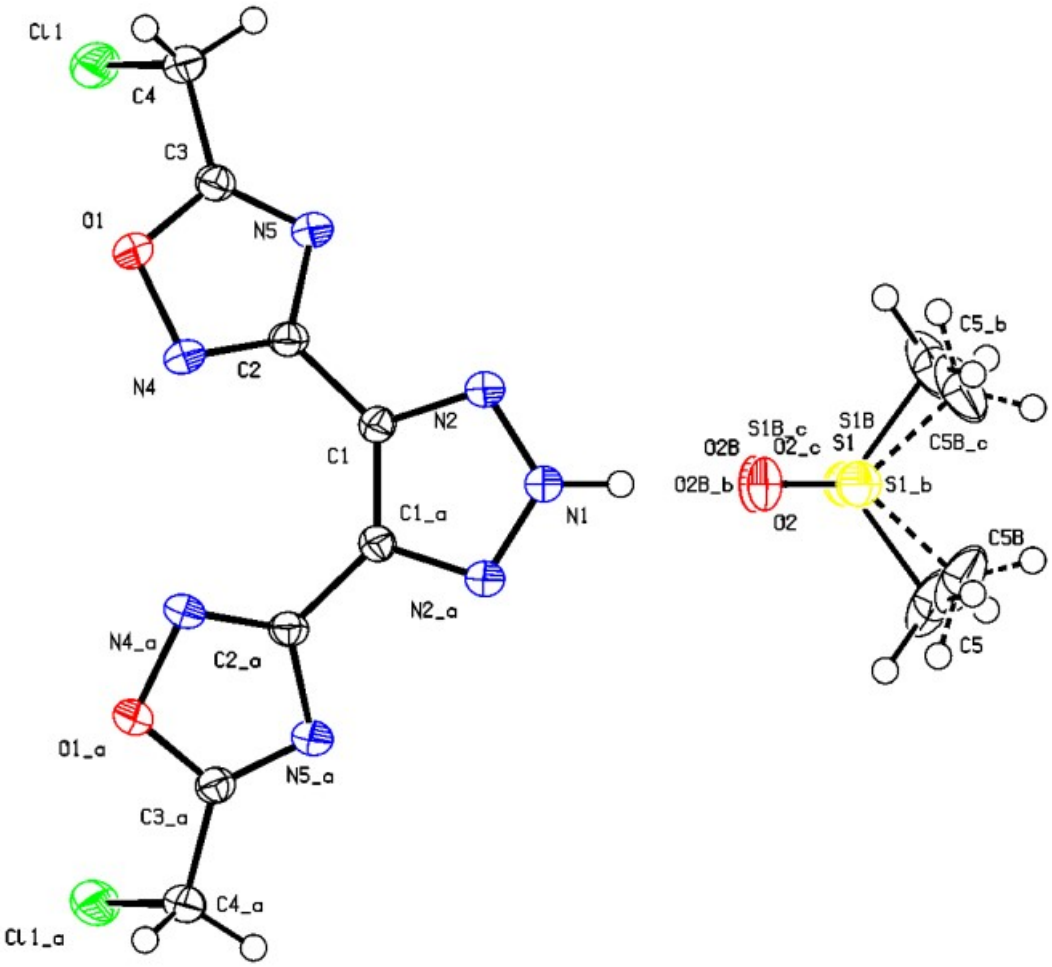

Fig. S02. Single crystal X-ray structure of compound **4·DMSO (**CCDC NO 2330491**).** Drawing of compound at 50% ellipsoids showing both orientations of the disordered DMSO.[6-10]

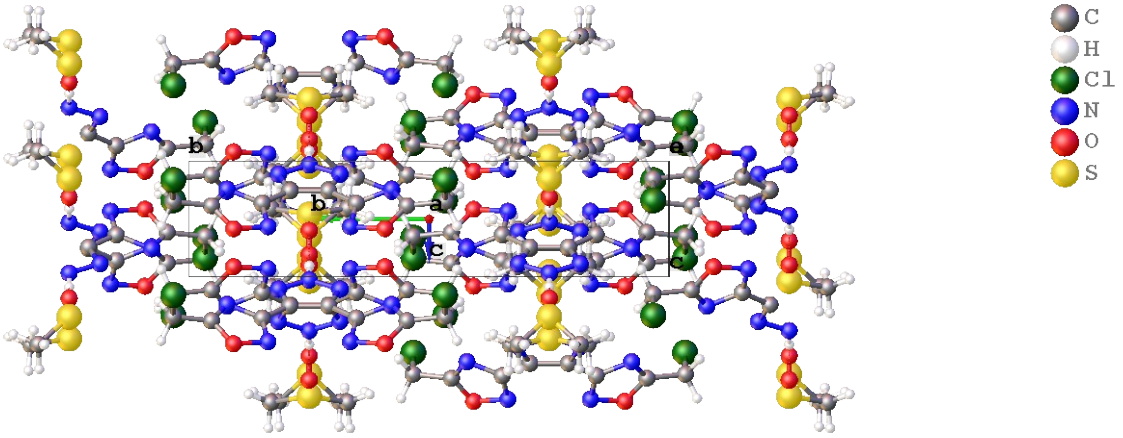

Fig. S03. Packing diagram of **4·DMSO** viewed along the **a** axis.[6-10]

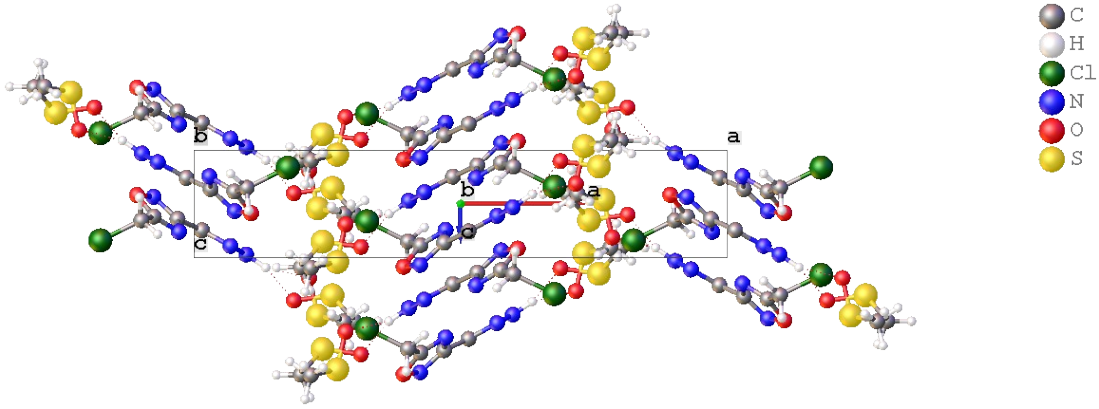

Fig. S04. Packing diagram of **4·DMSO** viewed along the **b** axis. [6-10]

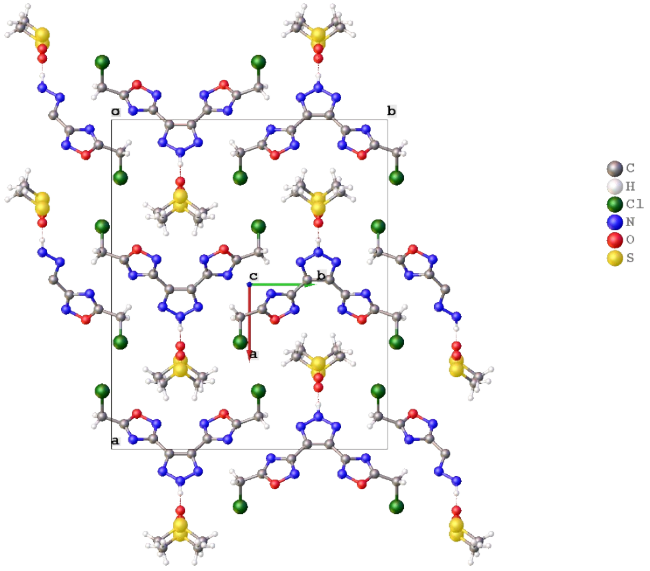

Fig. S05. Packing diagram of **4·DMSO** viewed along the **c** axis. [6-10]

Table S04: Bond Lengths in Å for **4·DMSO**.[6-10]

Atom	Atom	Length/Å
Cl1	C4	1.792(3)
O1	C3	1.343(3)
N1	N21	1.322(3)
N1	N2	1.322(3)
N2	C1	1.344(3)
N4	C2	1.297(3)
N5	C2	1.388(3)
N5	C3	1.285(3)
C1	C11	1.409(4)
C1	C2	1.463(3)
O1	N4	1.415(3)
C3	C4	1.493(3)
S1	O2B	1.510(4)
S1	C5	1.757(7)
S1	C51	1.757(7)
S1B	O2	1.525(11)
S1B	C5B1	1.733(17)
S1B	C5B	1.733(17)

Table S05: Bond Angles in ° for **4·DMSO**.[6-10]

Atom	Atom	Atom	Angle/°
C3	O1	N4	105.93(18)
N2	N1	N2[1]	116.2(3)
N1	N2	C1	103.8(2)
C2	N4	O1	102.96(18)
C3	N5	C2	101.8(2)
N2	C1	C1[1]	108.11(13)
N2	C1	C2	118.0(2)
C1[1]	C1	C2	133.82(13)
N4	C2	N5	115.1(2)
N4	C2	C1	124.5(2)
N5	C2	C1	120.4(2)
O1	C3	C4	117.8(2)
N5	C3	O1	114.2(2)
N5	C3	C4	127.9(2)
C3	C4	Cl1	109.40(17)
O2B	S1	C5	104.7(4)
C51	S1	C5	106.2(5)
O2	S1B	C5B1	113.9(16)
O2	S1B	C5B	113.9(16)
C5B1	S1B	C5B	81(2)

Table S06: Torsion Angles in ° for **4·DMSO**.[6-10]

Atom	Atom	Atom	Atom	Angle/°
O1	N4	C2	N5	0.6(3)
O1	N4	C2	C1	-179.2(2)
O1	C3	C4	Cl1	-67.3(3)
N1	N2	C1	C1[1]	-0.1(2)
N1	N2	C1	C2	-177.0(2)
N2[1]	N1	N2	C1	0.1(4)
N2	C1	C2	N4	-162.8(2)
N2	C1	C2	N5	17.4(4)
N4	O1	C3	N5	-0.4(3)
N4	O1	C3	C4	178.8(2)
N5	C3	C4	Cl1	111.7(3)
C1[1]	C1	C2	N4	21.2(3)
C1[1]	C1	C2	N5	-158.59(15)
C2	N5	C3	O1	0.7(3)
C2	N5	C3	C4	-178.4(3)
C3	O1	N4	C2	-0.2(3)
C3	N5	C2	N4	-0.8(3)
C3	N5	C2	C1	179.0(2)

Table S07: Hydrogen Bond information for **4·DMSO**.[6-10]

D	H	A	d(D-H)/Å	d(H-A)/Å	d(D-A)/Å	D-H-A/deg
N1	H1	O2B	0.93(6)	1.76(6)	2.645(5)	160(5)
N1	H1	O2	0.93(6)	1.70(6)	2.606(10)	164(5)

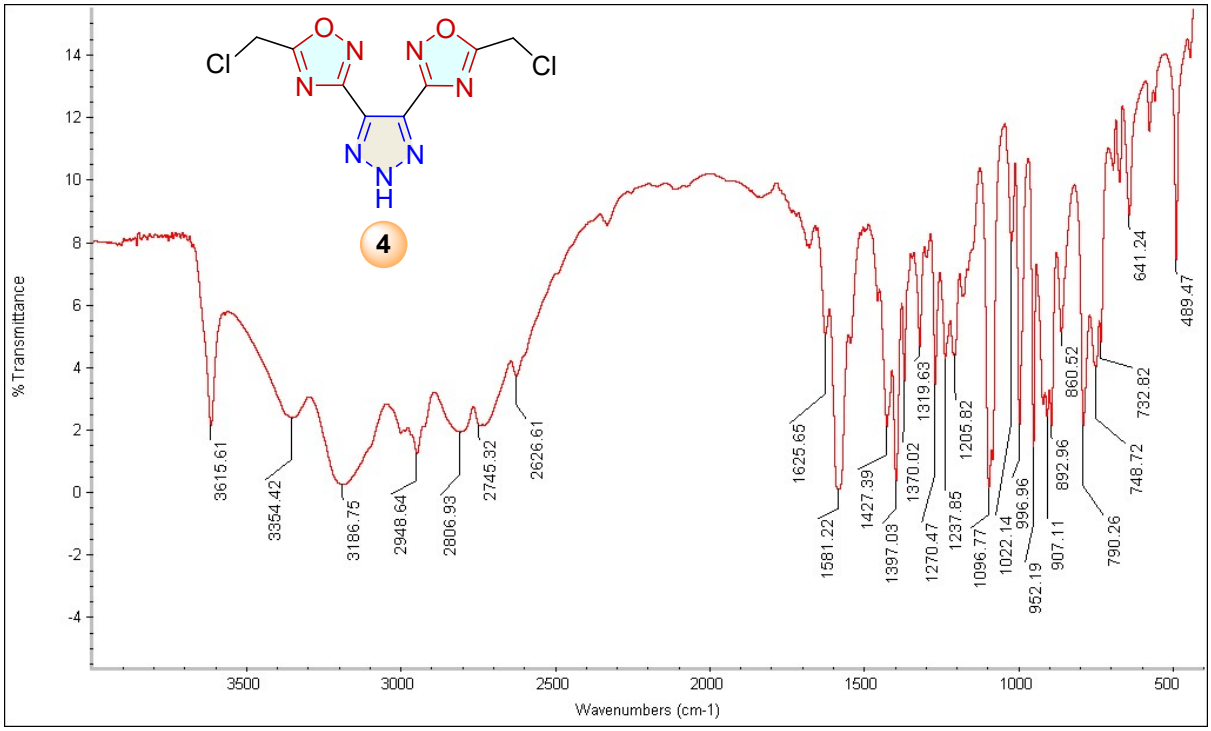

Fig. S06. FTIR-Spectrum of Compound **4**.

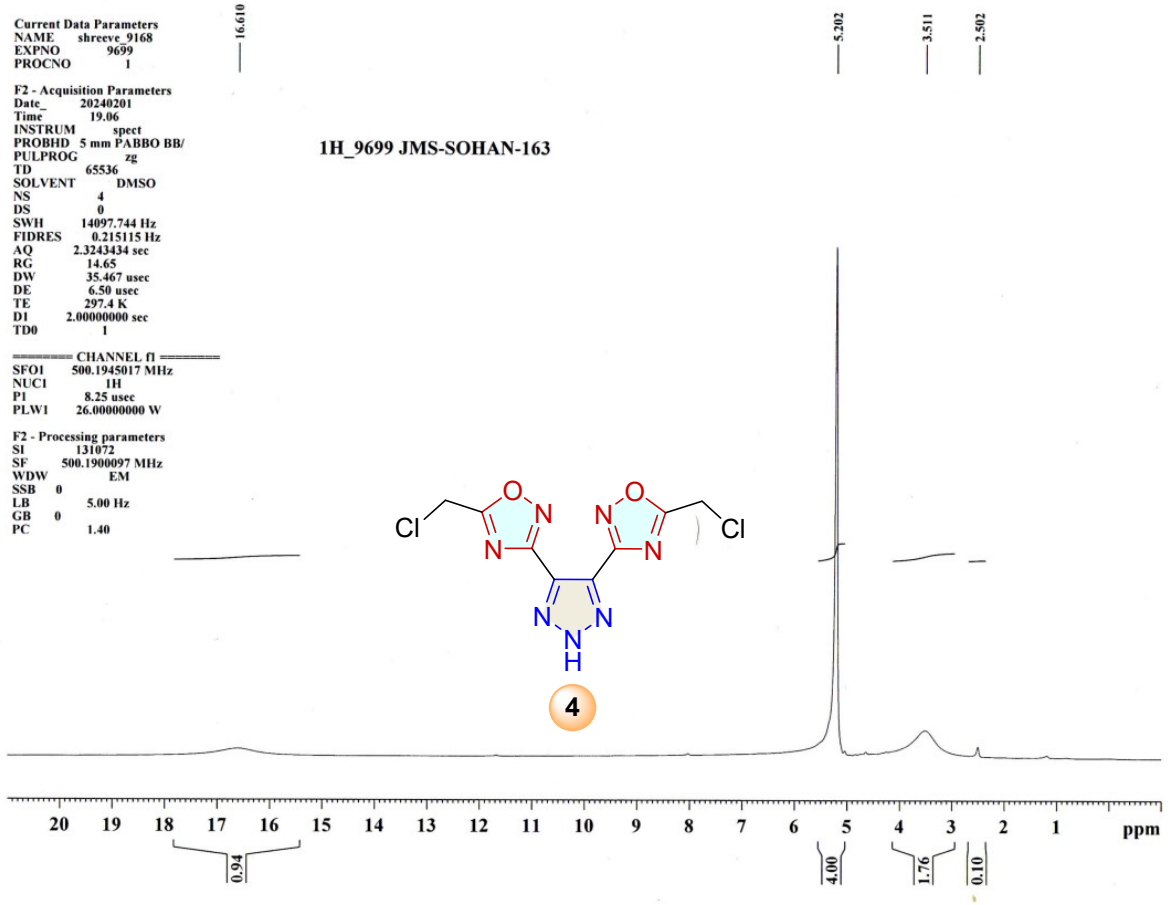

Fig. S07. ^{1}H NMR Spectrum of Compound **4** (500.19 MHz).

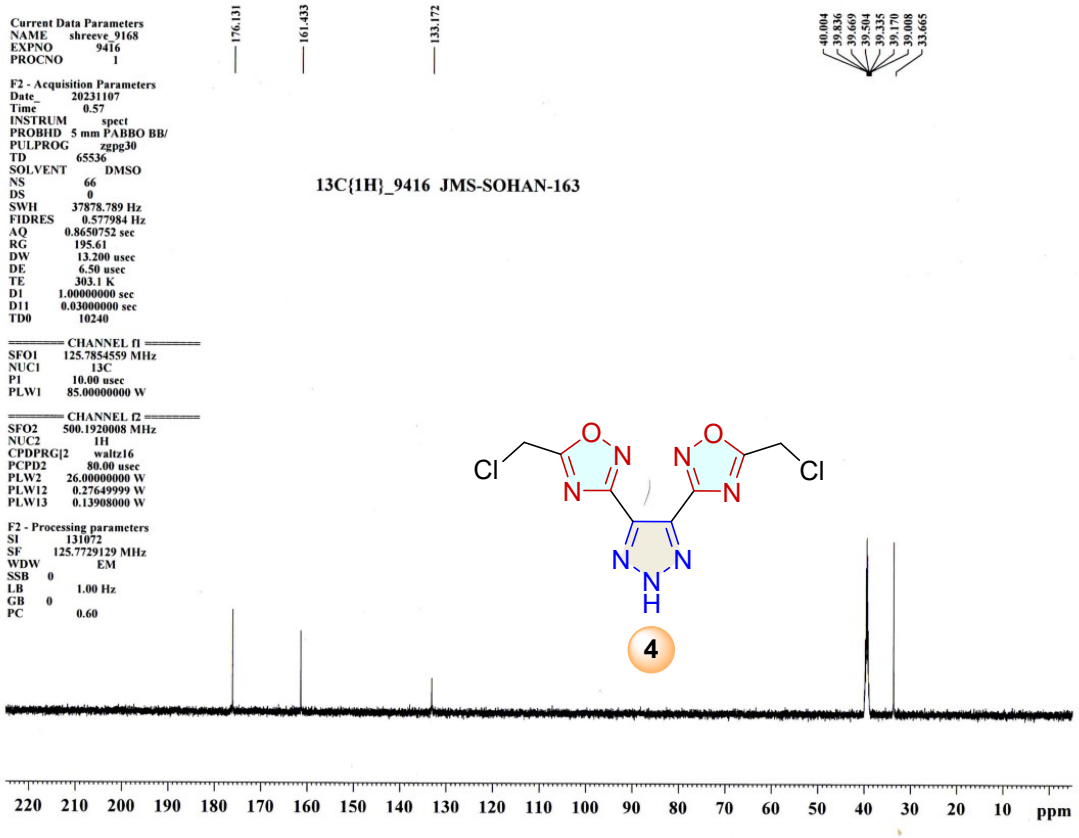

Fig. S08. ^{13}C NMR Spectrum of Compound **4** (125.77 MHz).

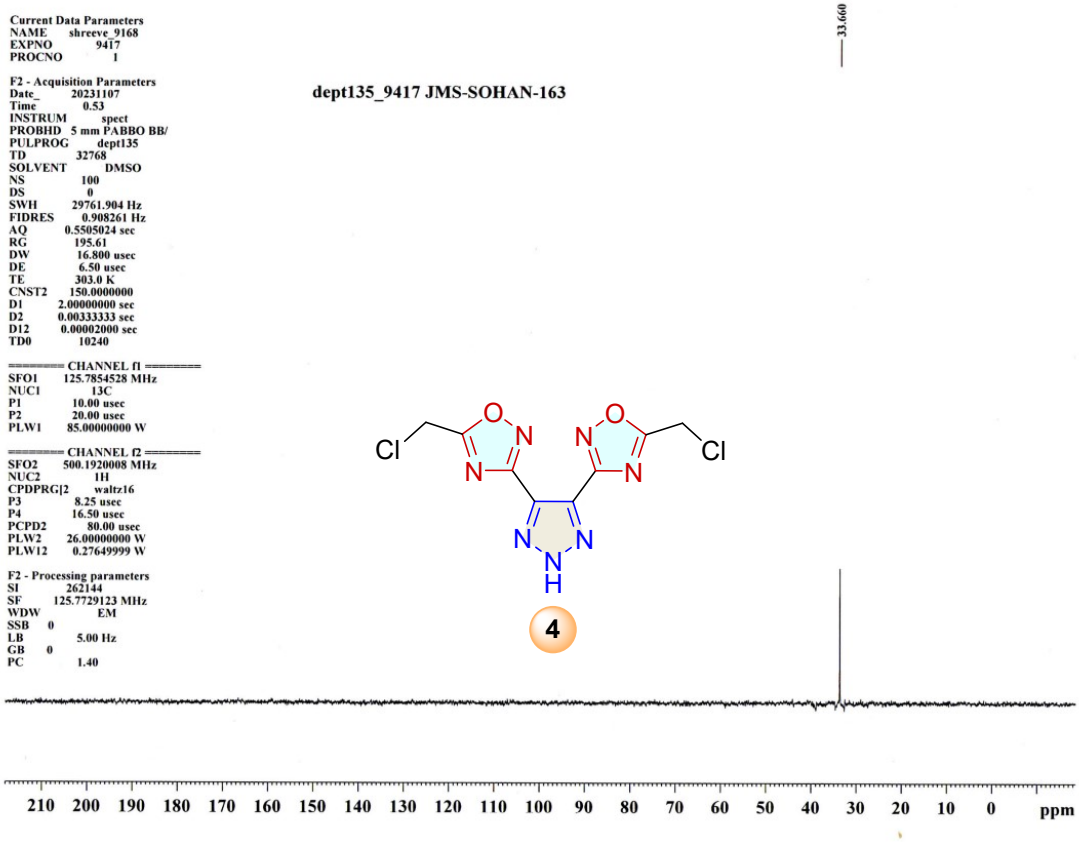

Fig. S09. ^{13}C-DEPT NMR Spectrum of Compound **4** (125.77 MHz).

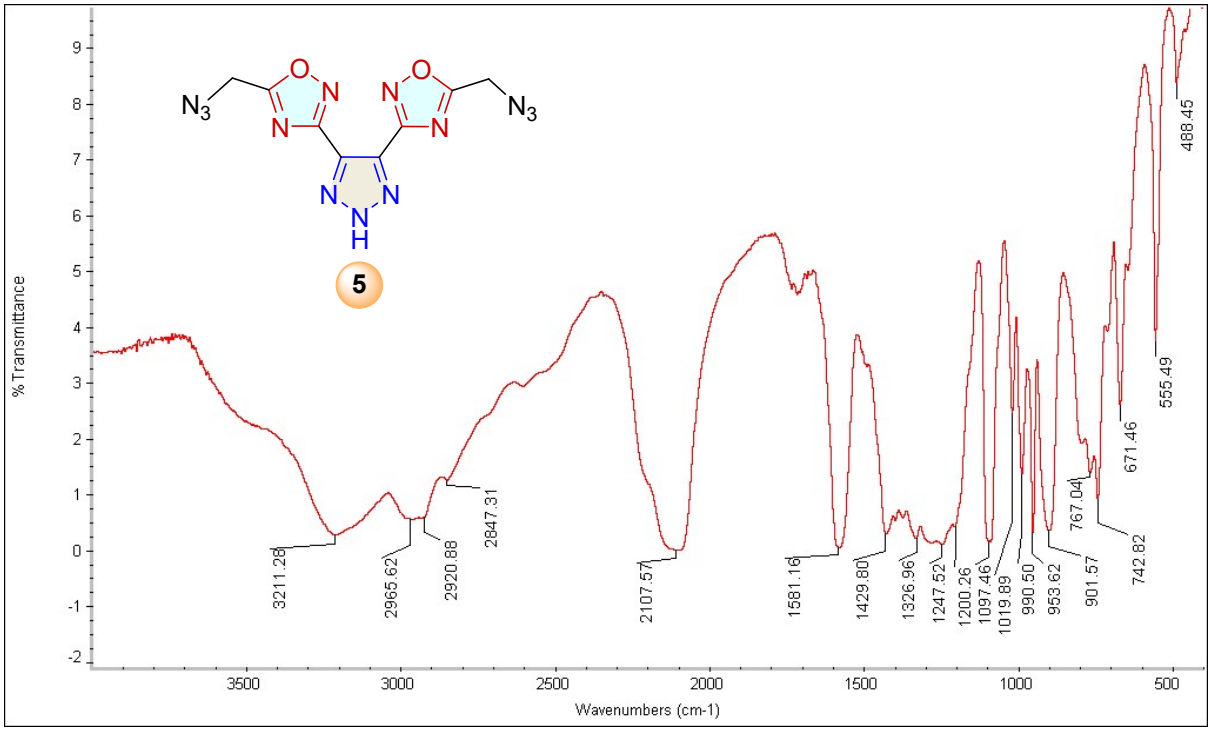

Fig. S10. FTIR-Spectrum of Compound **5**.

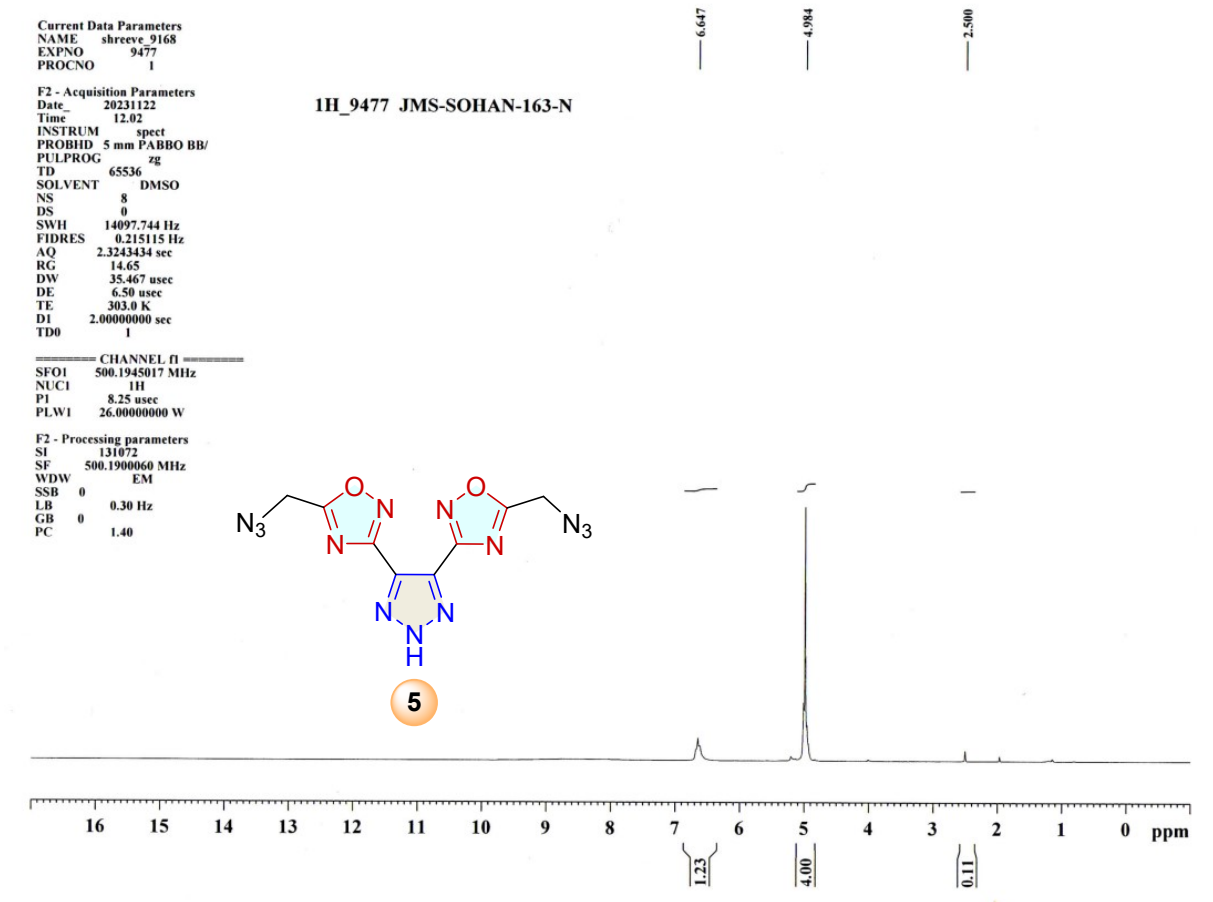

Fig. S11. ^{1}H NMR Spectrum of Compound **5** (500.19 MHz).

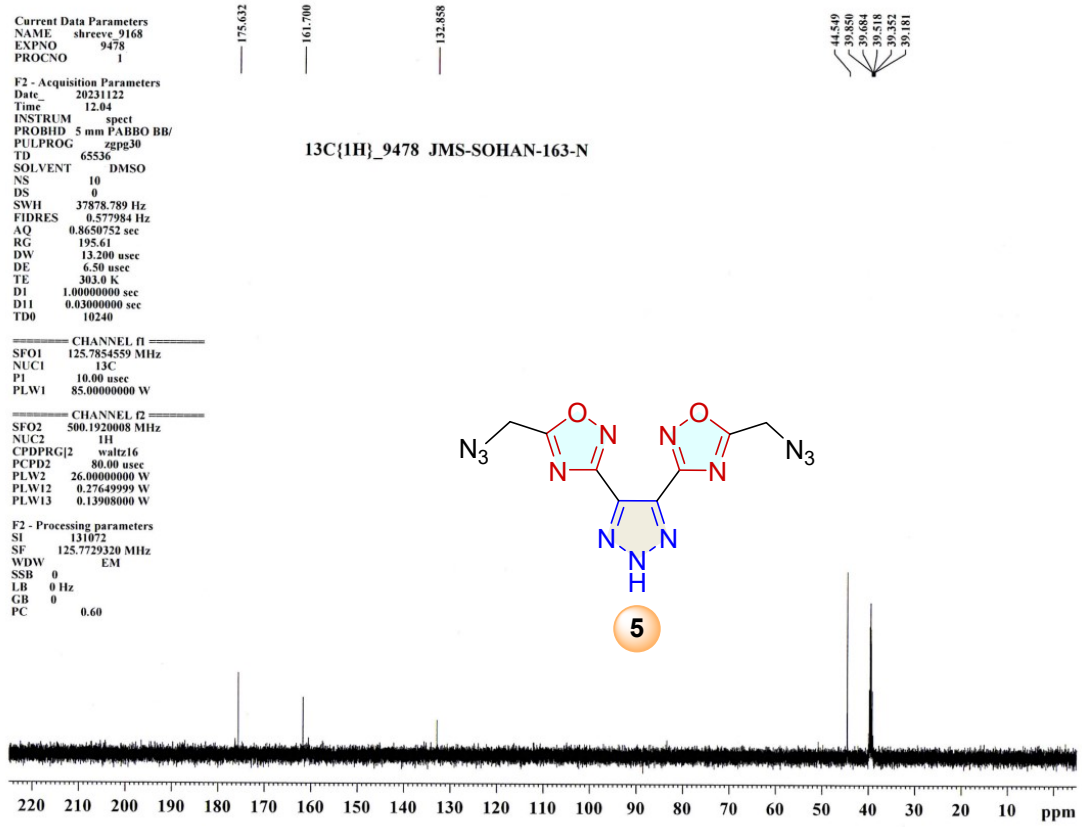

Fig. S12. ^{13}C NMR Spectrum of Compound **5** (125.77 MHz).

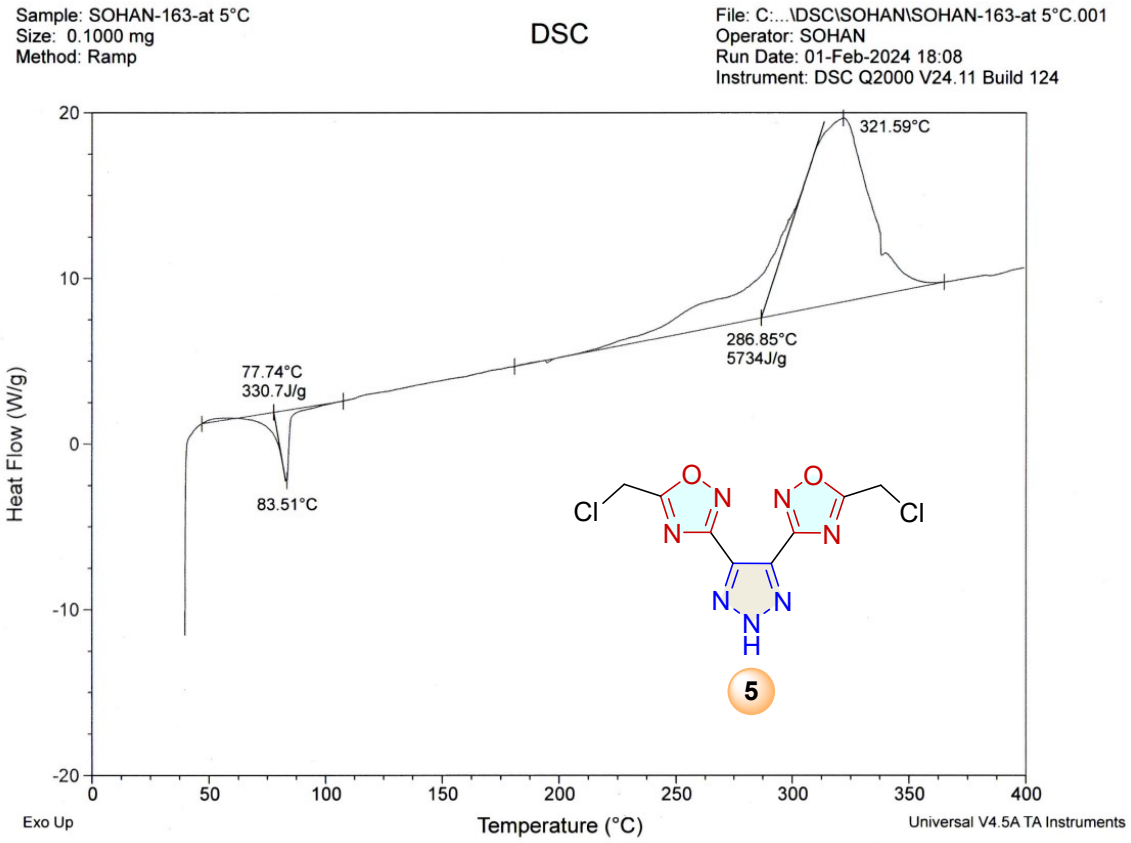

Fig. S13. DSC of compound **4** at 5 °C min^{-1}

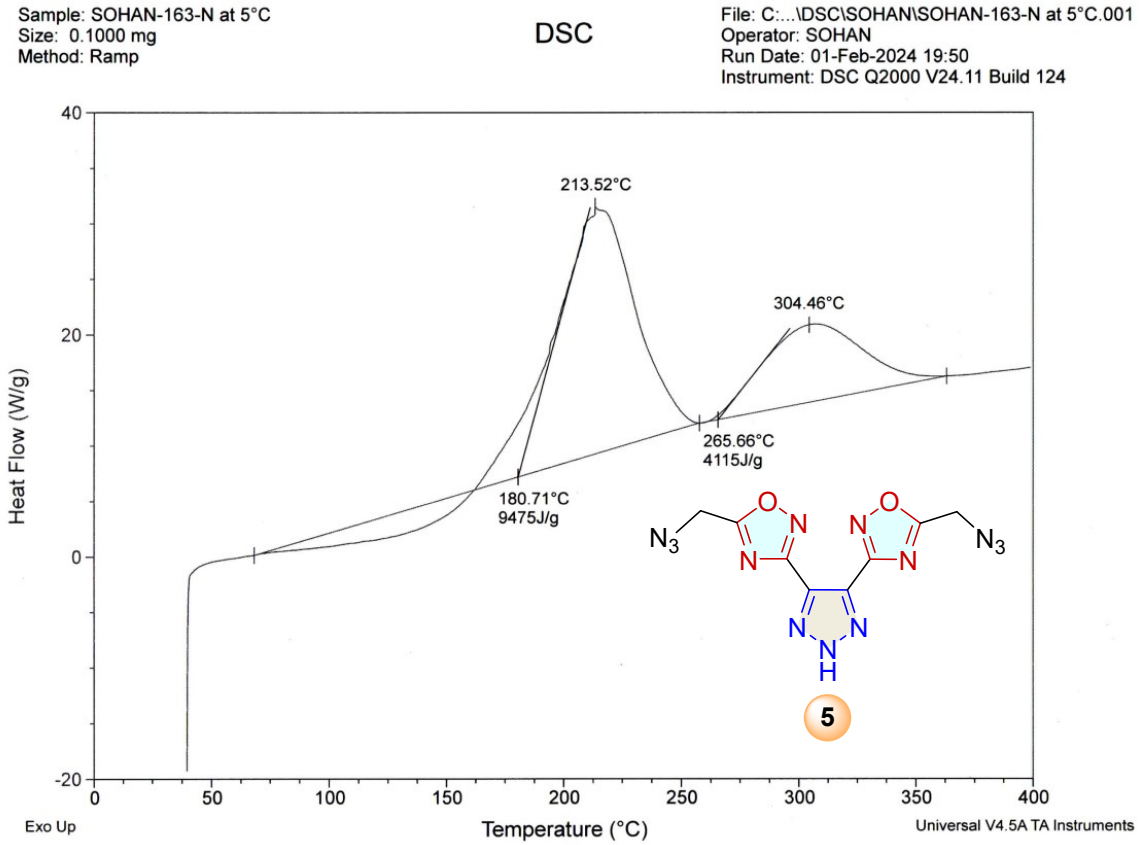

Fig. S14. DSC of compound **5** at 5 °C min^{-1}

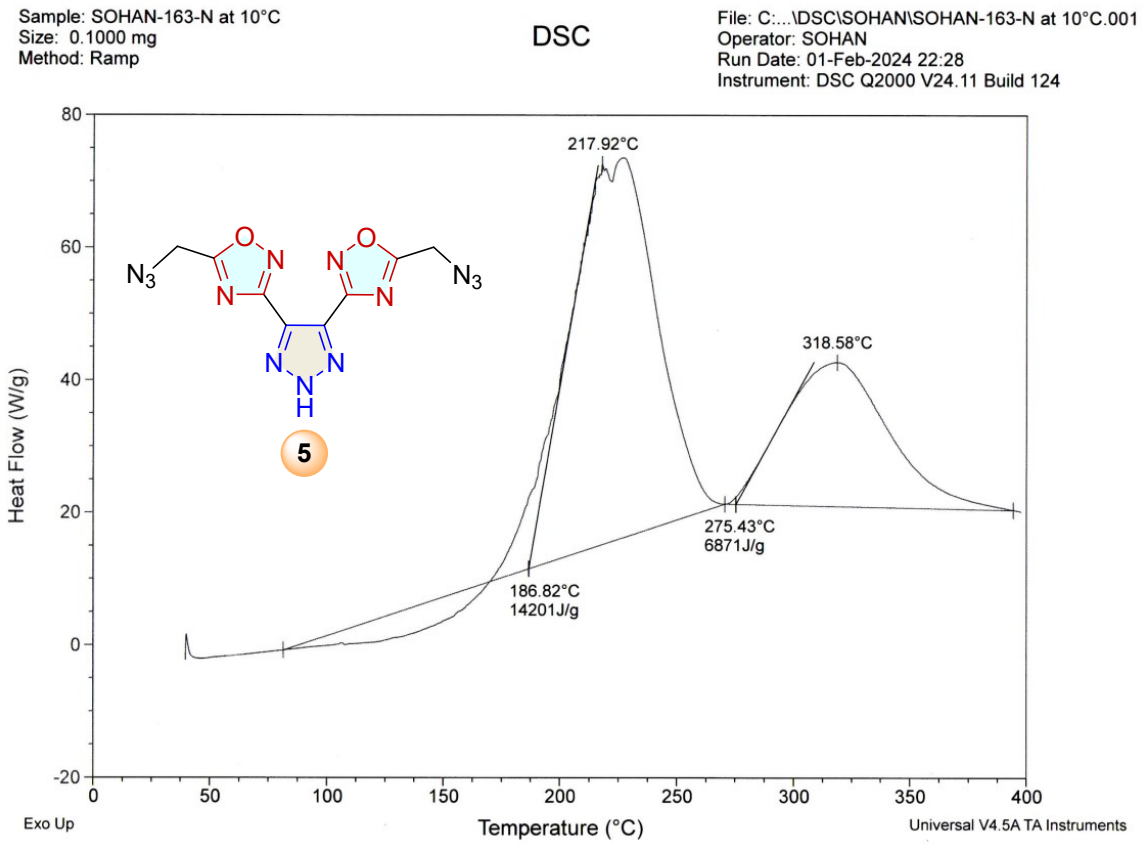

Fig. S15. DSC of compound **5** at 10 °C min^{-1}

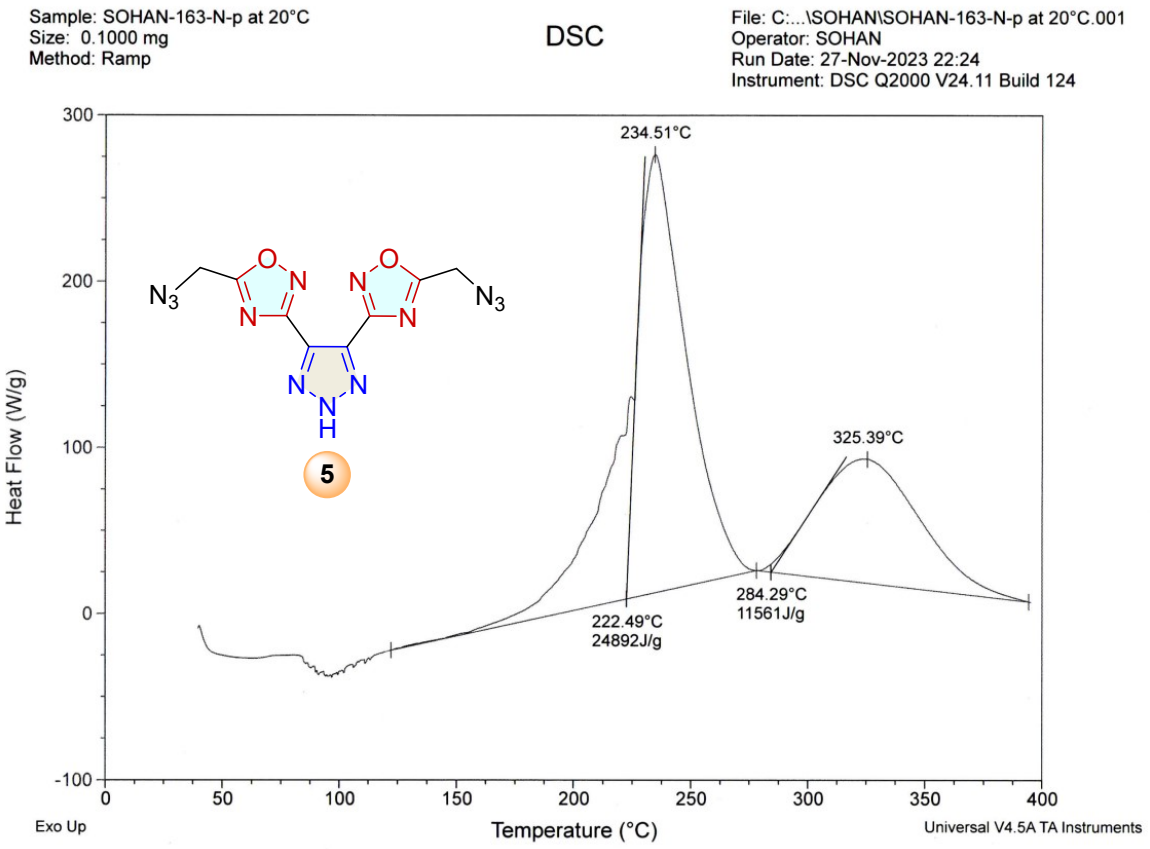

Fig. S16. DSC of compound **5** at 20 °C min^{-1}

Table S08. Atomic coordinates for optimized structure of compound **5** obtained using the B3LYP/6-311++G(d,p) level of theory.

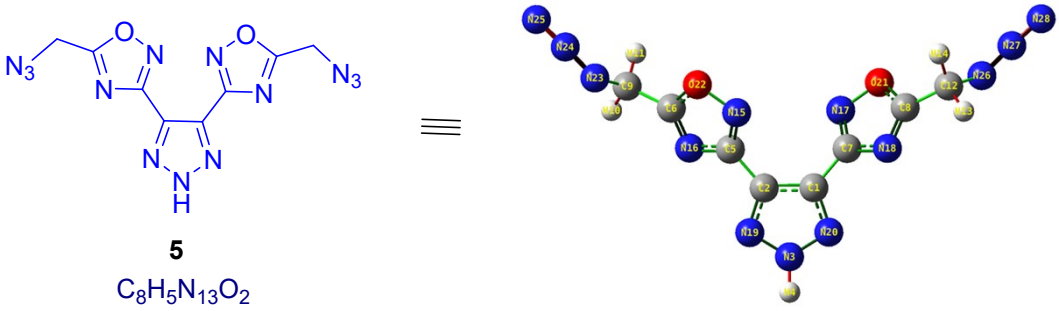

5

$C_8H_5N_{13}O_2$

MW = 315.22

optimized structure

```
Zero-point correction=                           0.175367 (Hartree/Particle)
Thermal correction to Energy=                    0.194685
Thermal correction to Enthalpy=                  0.195630
Thermal correction to Gibbs Free Energy=         0.118421
Sum of electronic and zero-point Energies=         -1169.946368
Sum of electronic and thermal Energies=            -1169.927050
Sum of electronic and thermal Enthalpies=          -1169.926106
Sum of electronic and thermal Free Energies=       -1170.003315
```

Center Number	Atomic Symbol	Coordinates (Angstroms) X	Y	Z
1	C	2.464031	-1.590444	-1.296804
2	C	2.878063	-0.239684	-1.176929
3	N	0.798273	-0.341582	-1.230794
4	H	-0.167217	-0.045966	-1.227894

5	C	4.215551	0.338368	-1.051059
6	C	5.827862	1.636970	-1.257297
7	C	3.248079	-2.818306	-1.428220
8	C	3.868654	-4.792337	-1.212597
9	C	6.799010	2.713119	-1.612546
10	H	6.270445	3.435140	-2.240038
11	H	7.620916	2.275567	-2.190890
12	C	4.084091	-6.222851	-0.846456
13	H	3.270573	-6.514399	-0.177341
14	H	5.035513	-6.315058	-0.310050
15	N	5.156159	-0.245708	-0.354316
16	N	4.592429	1.531449	-1.631520
17	N	4.335981	-2.866610	-2.152931
18	N	2.911685	-4.011230	-0.823168
19	N	1.788566	0.529335	-1.141096
20	N	1.130685	-1.617591	-1.324823
21	O	4.764259	-4.186361	-2.004537
22	O	6.245253	0.615200	-0.496946
23	N	7.297510	3.352681	-0.378595
24	N	8.388535	3.914832	-0.475947
25	N	9.378159	4.465569	-0.432978
26	N	4.082276	-7.047868	-2.071357
27	N	4.642594	-8.139963	-1.974825
28	N	5.123599	-9.165336	-2.017031

Number of imaginary frequencies at the B3LYP/6-311++G(d,p) level = 0

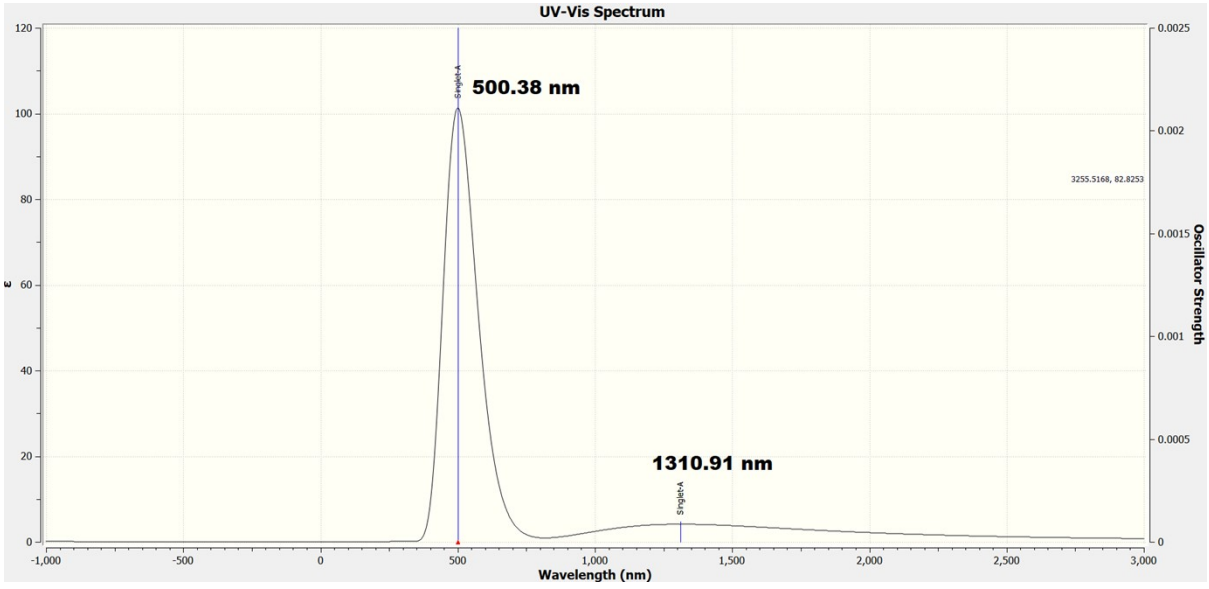

Fig. S17: Predicted UV-Visible spectrum of compound **5** at B3LYP/6-311++G(d,p) level.

References

1. M. J. Frisch, G. W. Trucks, H. B. Schlegel, G. E. Scuseria, M. A. Robb, J. R. Cheeseman, G. Scalmani, V. Barone, B. Mennucci, G. A. Petersson, H. Nakatsuji, M. L. Caricato, X., H. P. Hratchian, A. F. Izmaylov, J. Bloino, G. Zheng, J. L. Sonnenberg, M. Hada, M. Ehara, K. Toyota, R. Fukuda, J. Hasegawa, M. Ishida, T. Nakajima, Y. Honda, O. Kitao, H. Nakai, T. Vreven, J. A. Montgomery, Jr., J. E. Peralta, F. Ogliaro, M. Bearpark, J. J. Heyd, E. Brothers, K. N. Kudin, V. N. Staroverov, R. Kobayashi, J. Normand, K. Raghavachari, A. Rendell, J. C. Burant, S. S. Iyengar, J. Tomasi, M. Cossi, N. Rega, N. J. Millam, M. Klene, J. E. Knox, J. B. Cross, V. Bakken, C. Adamo, J. Jaramillo, R. Gomperts, R. E. Stratmann, O. Yazyev, A. J. Austin, R. Cammi, C. Pomelli, J. W. Ochterski, R. L. Martin, K. Morokuma, V. G. Zakrzewski, G. A. Voth, P. Salvador, J. J. Dannenberg, S. Dapprich, A. D. Daniels, Ö. Farkas, J. B. Foresman, J. V. Ortiz, J. Cioslowski and D. J. Fox, Revision D.01 ed., Gaussian, Inc., Wallingford, CT, 2003.
2. P. W. Atkins, Physical Chemistry, Oxford University press: Oxford 1982.
3. M. S. Westwell, M. S. Searle, D. J. Wales and D. H. Williams, Empirical correlations between thermodynamic properties and intermolecular forces, *J. Am. Chem. Soc.,* 1995, **117**, 5013–5015
4. H. Gao, C. Ye, C. M. Piekarski and J. M. Shreeve, Computational characterization of energetic salts, *J. Phys. Chem. C,* 2007, **111**, 10718–10731.
5. T. M. Klapötke, Chemistry of High Energy Materials, 6th Edn., Walter de Gruyter, Berlin/Boston, 2022.
6. G. M. Sheldrick, Crystal structure refinement with SHELXL, *Acta Crystallogr. Sect. A Found. Adv.*, 2015, **C71**, 3-8.
7. G. M. Sheldrick, A short history of *ShelX, Acta Cryst.,* 2008, ***A64***, 112-122.
8. Twin reference: S. Parsons, Introduction to twinning *Acta Cryst.,* 2003, **D59**, 1995-2003.
9. (a) CrysAlisPro Software System, Rigaku Oxford Diffraction, 2020. (b) G. M. Sheldrick, ShelXT-Integrated space-group and crystal-structure determination, *Acta Cryst*., 2015, **A71**, 3-8.
10. O. V. Dolomanov, L. J. Bourhis, R. J. Gildea, J. A. K. Howard and H. Puschmann, OLEX2 A complete structure solution, refinement and analysis program. *J. Appl. Crystallogr.,* 2009, **42**, 339-341.